Evolved Peroxygenase-Aryl Alcohol Oxidase Fusions for Self-Sufficient Oxyfunctionalization Reactions

Gomez De Santos, Patricia; Lazaro, Sofia; Viña-Gonzalez, Javier; Hoang, Manh Dat; Sánchez-Moreno, Israel; Glieder, Anton; Hollmann, Frank; Alcalde, Miguel

DOI
10.1021/acscatal.0c03029

Publication date
2020

Document Version
Final published version

Published in
ACS Catalysis

ACS Catalysis

pubs.acs.org/acscatalysis

Research Article

Evolved Peroxygenase–Aryl Alcohol Oxidase Fusions for Self-Sufficient Oxyfunctionalization Reactions

Patricia Gomez de Santos, Sofia Lazaro, Javier Viña-Gonzalez, Manh Dat Hoang, Israel Sánchez-Moreno, Anton Glieder, Frank Hollmann, and Miguel Alcalde*

Cite This: *ACS Catal.* 2020, 10, 13524–13534

Read Online

ACCESS | Metrics & More | Article Recommendations | Supporting Information

ABSTRACT: Fungal peroxygenases are deemed emergent biocatalysts for selective C–H bond oxyfunctionalization reactions. In this study, we have engineered a functional and stable self-sufficient chimeric peroxygenase-oxidase fusion. The bifunctional biocatalyst carried a laboratory-evolved version of the fungal peroxygenase fused to an evolved fungal aryl-alcohol oxidase that supplies H_2O_2 *in situ*. Enzyme fusion libraries with peptide linkers of different sizes and amino acid compositions were designed, while attached leader sequences favored secretion in yeast. The most promising functional enzyme fusions were characterized biochemically and further tested for the synthesis of dextrorphan, a metabolite of the antitussive drug dextromethorphan. This reaction system was optimized to control the aromatic alcohol transformation rate, and therefore the H_2O_2 supply, to achieve total turnover numbers of 62,000, the highest value reported for the biocatalytic synthesis of dextrorphan to date. Accordingly, our study opens an avenue for the use of peroxygenase-aryl alcohol oxidase fusions in the pharmaceutical and chemical sectors.

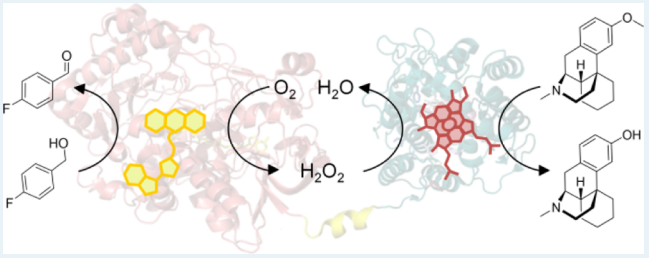

KEYWORDS: *enzyme fusion, unspecific peroxygenase, aryl alcohol oxidase, in situ H_2O_2 generation, human drug metabolites*

INTRODUCTION

Fungal unspecific peroxygenases (UPOs; EC 1.11.2.1) are a group of heme-thiolate enzymes that perform C–H bond oxyfunctionalization reactions with high selectivity, triggered simply by H_2O_2 that serves as the final electron acceptor and the oxygen donor. A wide repertoire of two-electron oxidation (mono(per)oxygenation) reactions are carried out by UPO, including aromatic and alkyl hydroxylations, aromatic and aliphatic epoxidations, N-dealkylations, O-dealkylations (including ester and ether cleavage), S-oxidations, N-oxidations, and brominations.[1,2] Indeed, UPOs are considered versatile biocatalysts with a large portfolio of oxyfunctionalization reactions that appeal to both the chemical and pharmaceutical sectors.[3−6] In particular, the use of UPOs in the synthesis of human drug metabolites (HDMs) is of great relevance, a fundamental aspect of pharmacokinetic and pharmacodynamic studies in the drug development pipeline.[4]

Unfortunately, the poor oxidative stability of UPOs (*i.e.*, its rapid and irreversible inactivation by catalytic concentrations of H_2O_2) represents the "Achilles heel" of this nascent industrial biocatalyst. This complex problem is being studied actively, applying different strategies that combined peroxygenases with photo-, electro-, and chemocatalysis, as well as using enzyme cascade reactions, all of which aim to control the supply of H_2O_2 *in situ*.[7−20] However, designing a self-sufficient peroxygenase in which the desired mono(per)oxygenase activity is coupled to a direct stoichiometric feed of H_2O_2 generated by a H_2O_2-producing oxidase, within the same polypeptide chain, could represent a breakthrough in this field. Indeed, compared to the aforementioned methods of generating H_2O_2, a chimeric peroxygenase-oxidase fusion protein seems to be the simplest and most flexible approach, which may streamline experimental work and resources. The proximity of the two different catalytic sites may help to control the direct release and diffusion of H_2O_2 (substrate channeling effect), increasing oxyfunctionalization reaction rates while limiting oxidative damage.[21−23] More significantly, this chimeric peroxygenase-oxidase fusion could allow one-pot, two-step cascade reactions or the production of two valuable compounds in one single reaction.[23] It is well known that in conventional biocatalysis with H_2O_2-producing oxidases, O_2 is not used efficiently as it is reduced to H_2O_2, forming this useless byproduct, whereas with the proposed enzyme fusion, O_2 could be reduced twice, as the byproduct of the oxidase activity represents the main fuel for peroxygenase, allowing both oxidations—by the oxidase- and C–H oxyfunctionalization reactions—by the peroxygenase. In the long term and

Received: July 10, 2020
Revised: October 21, 2020
Published: November 5, 2020

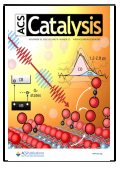

https://dx.doi.org/10.1021/acscatal.0c03029
ACS Catal. 2020, 10, 13524–13534

Table 1. Fusion Library I[a]

construct	leader sequence	N-terminal partner	linker	C-terminal partner	UPO activity[b]	AAO activity[b]	UPO_AAO activity[b]
A	evSp	UPO	$LA(EAAAK)_4AAA$	AAO	++		
B	evSp	UPO	$LA(EAAAK)_5AAA$	AAO	++		
B′	evSp	UPO	$LA(EAAAK)_5$ $AAA(GGGGR)_1$	AAO	+++	+++	+++
C	preαproK	AAO	$(GGGGR)_1$ $LA(EAAAK)_4AAA$	UPO		+	
D	preαproK	AAO	$(GGGGR)_1$ $LA(EAAAK)_5AAA$	UPO		+	

[a]The order of the enzymes, and the leader sequences and linkers used are indicated. [b]Activity was measured in supernatants of independent cultures grown in 96-well plates using the ABTS/H_2O_2 assay for UPO, the 4-methoxybenzyl alcohol/ABTS-HRP-coupled assay for AAO, or the 4-methoxybenzyl alcohol/ABTS assay for the UPO_AAO fusion, see also Figure 1. Each construct contained a leader sequence, followed by the two enzyme partners connected by a linker, and they were measured in independent 96-well cultures.

given that the production of H_2O_2 and mono(per)oxygenase activity could be unified within a single polypeptide, the bifunctional biocatalyst formed by the fusion of these two independent enzymes could thereafter be subjected to directed coevolution in order to adapt it to meet specific industrial demands.

We chose a natural UPO partner to design a self-sufficient peroxygenase-oxidase fusion, the aryl-alcohol oxidase (AAO; EC 1.1.3.7). As a monomeric extracellular flavoprotein, fungal AAO oxidizes a wide range of aromatic alcohols to their corresponding carbonyl compounds, producing H_2O_2 as the only byproduct.[24] With common occurrences and complementary functions, both AAO and UPO act in nature within the group of fungal ligninolytic oxidoreductases—also referred to as ligninases—, a consortium of enzymes that also includes high-redox potential laccases and peroxidases, being responsible for the degradation of recalcitrant lignin in plants.[25,26] Generally speaking, ligninases are precious biocatalysts with a range of applications in environmental biocatalysis, from bioremediation to novel green processes, yet their engineering is in practice extremely difficult because of the complications associated with their functional expression in heterologous hosts, for which AAO and UPO are no exception.[27] The absence of chaperones and of different post-translational modifications (glycosylation, disulfide bridge, and N- and C-terminal processing) are important hurdles that must be circumvented.[28−30] As such, the directed evolution of ligninases to improve their heterologous functional expression is crucial for future design efforts. We previously carried out several directed evolution campaigns in order to improve the functional expression of UPO and AAO in yeast (*Saccharomyces cerevisiae* and *Pichia pastoris*) and subsequently for the synthesis of HDMs and secondary aromatic alcohols.[31−42]

Here, as our departure point, we selected two evolved variants of UPO and AAO to design a collection of secreted functional UPO_AAO fusion enzymes. An array of peptide linkers of different lengths and amino acid compositions, together with different evolved leader sequences, were used to construct functional libraries of the chimeric UPO_AAO fusions. The best designs were produced, purified, and characterized biochemically. As a proof of concept of the worth of such a bifunctional biocatalyst, the fusions generated were studied in the synthesis of the true HDM from the drug dextromethorphan, an antitussive agent with sedative and dissociative properties.

RESULTS AND DISCUSSION

Point of Departure to Construct the Chimeric Fusion Enzymes: Laboratory-Evolved AAO and UPO Variants. We previously generated several secretion mutants by laboratory evolution of the AAO from *Pleurotus eryngii* and the UPO from *Agrocybe aegerita*. These evolved enzymes are highly active, stable, and functionally expressed at reasonable titers in yeast, which make them suitable templates for the design of UPO_AAO fusions. The FX9 mutant was used as the AAO partner, which was the product of five rounds of directed, structure-guided evolution to enhance its functional expression: 4 mg L^{-1} in *S. cerevisiae* and ∼25 mg L^{-1} in *P. pastoris* in a fed-batch bioreactor.[34,40] FX9 carries the mutations F[3]S-N[25]D-T[50]A-F[52]L-H91N-L170M, of which the mutations in the chimeric leader sequence preαproK that promoted secretion are underlined.[40] Concerning UPO, we chose the SoLo variant, which shows a reduced peroxidase activity *versus* several aromatic alcohols as a result of three consecutive directed evolution campaigns: (i) for secretion by yeast, achieving titers of 8 mg L^{-1} by *S. cerevisiae* and over 200 mg L^{-1} by *P. pastoris* in a bioreactor,[37,39] (ii) for production of the agrochemical 1-naphthol,[38] and (iii) for HDM synthesis.[31,32,43] Accordingly, SoLo carries the F[12]Y-A[14]V-R[15]G-A[21]-D-V[57]A-L67F-V75I-F191S-G241D-I248V-R257K-F311L mutations, the underlined residues lying in the evolved signal peptide (evSp).

Construction of the Enzyme Fusion Libraries. There are three key issues to consider when constructing enzyme fusions: the component partner enzymes, the connections between them, and their order in the fusion protein. The enzymatic partners were chosen in terms of their cooperative activity; in this case, UPO playing the leading role as the oxyfunctionalization partner and AAO playing the supporting role in the generation of H_2O_2. Rather than directly connecting UPO to AAO, that is, placing the genes together without a stop codon, we inserted a peptide linker to connect one to the other in order to avoid misfolding and/or loss of expression.[44,45] Given that not only the specific amino acids in this linker but also its length may be crucial, we focused on both flexible and rigid linkers of different sizes and compositions. Flexible linkers allow some degree of movement between the enzyme partners and they are mainly composed of repetitive stretches of small or hydrophilic amino acids such as Gly. By contrast, rigid linkers are stiff structures (*e.g.*, α-helical structures or multiple Pro residues) that may separate functional domains more efficiently, albeit with a loss of flexibility.[46]

As the fusion must be exported by yeast cells, the choice of a leader sequence that drives adequate secretion is also important. Accordingly, we designed four constructs (A, B, C, and D) to compare the secretion driven by both the evolved leader sequences, preαproK from AAO and evSp from UPO, as well as the effect of the different linkers on the expression of each fusion in distinct orientations, Table 1. The different

https://dx.doi.org/10.1021/acscatal.0c03029
ACS Catal. 2020, 10, 13524−13534

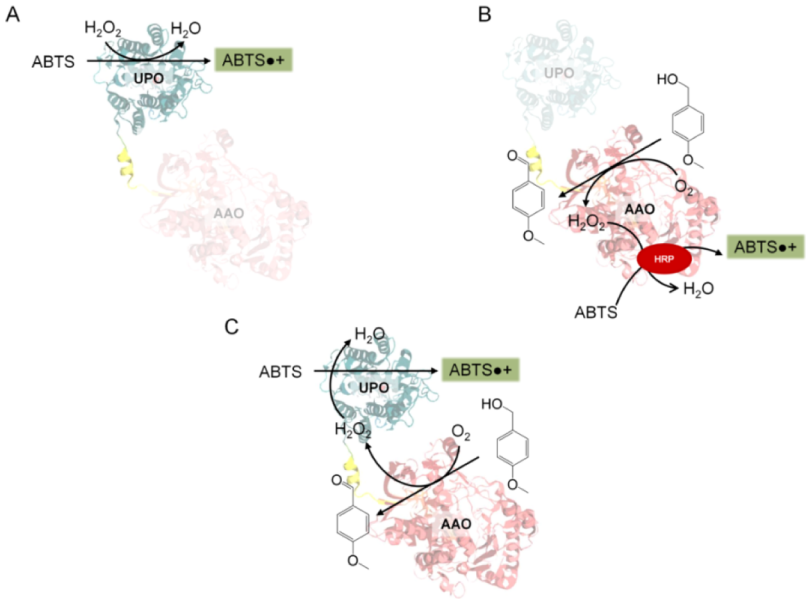

Figure 1. Screening of enzyme fusions. (A) ABTS/H_2O_2 assay. (B) 4-Methoxybenzyl alcohol/ABTS-HRP-coupled assay. (C) 4-Methoxybenzyl alcohol/ABTS assay. Assays A and B uncouple the activity of AAO or UPO, respectively, whereas assay C allows the activity of the whole fusion to be assessed. Assay B is performed in 100 mM phosphate buffer at pH 6.0, where the UPO's activity toward ABTS is not detectable (see the Materials and Methods section for details).

constructs were cloned *in vivo* into *S. cerevisiae* and screened for UPO activity using the ABTS/H_2O_2 assay, for AAO activity with the 4-methoxybenzyl alcohol/ABTS-HRP-coupled assay, and for both AAO and UPO activities with the 4-methoxybenzyl alcohol/ABTS assay, Figure 1.

The A and B constructs carried the evSp leader, followed by the UPO gene, which was joined to the AAO gene by a rigid linker of 25 (A construct) or 30 (B construct) amino acids. By contrast, in constructs C and D, the preαproK leader preceded the AAO gene, which was connected to the UPO gene by a linker that combined flexible and rigid regions of 30 (C construct) and 35 (D) amino acids. Constructs A and B displayed UPO activity but no AAO activity, whereas some AAO activity was detected for the C and D constructs, suggesting that a linker with a flexible region connected to the N-terminal domain of AAO may be important to maintain the AAO functional.

Indeed, this might protect the H-bonding between the FAD cofactor and the N-terminal of the AAO, which is crucial for the correct AAO folding.[47] Accordingly, we designed a new construct B′, which was similar to B but that included a flexible linker ending (GGGGR). For this construct, we analyzed different linker lengths: as the distance between the partners is important, the number of repetitions in the linker regions was explored by harnessing the high frequency of homologous DNA recombination in *S. cerevisiae*. In this way, the linker sequence was designed so that the yeast's DNA recombination machinery was prone to generate a library of fusions *in vivo* that contains linkers with different numbers of amino acid repetitions, Figure S1. This strategy was successful, and after screening the library, we identified a construct B′ UPO_AAO fusion with both activities that were coupled by a linker of 110 residues $(LA(EAAAK)_{20}AAA(GGGGR)_1)$. When this fusion was purified, three active fractions were isolated that corresponded to the UPO, AAO, and UPO_AAO fusion activity. The existence of these fractions indicated that the linker was attacked by proteases, possibly in the Golgi compartment, where *STE13*, a membrane-bound dipeptidyl aminopeptidase, can cleave the EA motifs.[48] This problem was solved by constructing a second library of UPO_AAO fusions in which the linker did not have cleavage sites for Golgi proteases, while still promoting possible recombination mismatches in the linkers to adjust their length (constructs E and F) and conserving a flexible region to connect to the N-terminal AAO, Table 2.

Table 2. Linkers Tested in Library II of the UPO_AAO Fusions

constructs[a]	linker	source
E	$(G)_8$	46
F	$(GGGGS)_3$	49
G	$(AP)_5(GGGGS)_1$	46
H	$(AP)_{15}(GGGGS)_2$	46
I	GTPTPTPTPTGEF	50
J	$GTPTPTPTPTGEF(GGGGS)_1$	50
K	FFALLNDPRG	linker database[51]
L	AVTYKKEEDL	linker database[51]

[a]All fusions were preceded by evSp, with UPO and AAO hierarchically connected by linkers of different characteristics: the E and F linkers were selected to test different degrees of flexibility; the G and H linkers included the AP rigid motif to confer a semirigid linkage between the partners; linker I proved to be tolerant to proteases; J is a modified version of I including a flexible region; and K and L are natural linkers from the vanadium peroxygenase from *Curvularia inaequalis*.

After screening fusion library II, we identified 10 functional fusion constructs with both UPO and AAO activities, Figure 2. The *in vivo* DNA recombination and assembly of the fusion in *S. cerevisiae* led to the isolation of four different F fusions whose activity was directly proportional to the increasing length of the linker: F4 $(GGGGS)_4$, F9 $(GGGGS)_9$, F12 $(GGGGS)_{12}$, and F17 $(GGGGS)_{17}$.

https://dx.doi.org/10.1021/acscatal.0c03029
ACS Catal. 2020, 10, 13524−13534

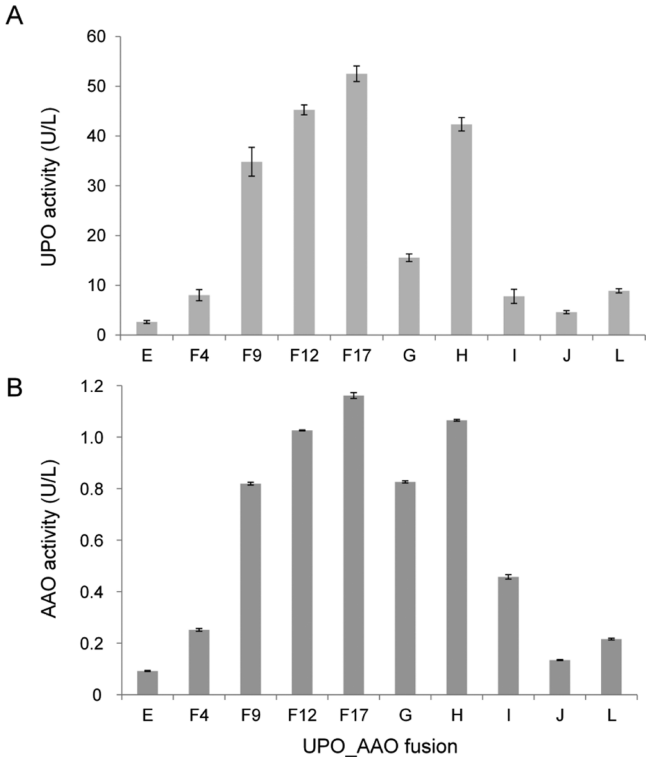

Figure 2. Activity of UPO_AAO fusions. (A) UPO activity and (B) AAO activity. The activity was measured in quintuplet from the supernatants of independent cultures using the ABTS/H_2O_2 assay for UPO and the 4-methoxybenzyl alcohol/ABTS-HRP-coupled assay for AAO. No activity of the K construct was detected.

Production and Biochemical Characterization. The five best constructs (F9, F12, F17, G, and H) were produced, purified, and characterized biochemically. Kinetic thermostability was determined by measuring the T_{50} (the temperature at which the enzyme retains 50% of its initial activity after a 10 min incubation). Thermostability was mostly conserved in all the fusions, with T_{50} values ranging from 57.3 to 58.8 °C *versus* 59.5 and 63 °C for free UPO and AAO, respectively (see the Materials and Methods section for details). All fusions were hyperglycosylated by yeast, with sugar moieties constituting roughly 50% of the molecular mass of the enzymes, Figure 3A. This was not surprising given that the molecular masses of individual UPO and AAO secreted by yeast are 52,000 and 150,000 Da, of which hyperglycosylation represents 30 and 60%, respectively.[31,34] The addition of outer-chain mannose moieties to complex and large proteins in the Golgi apparatus occurs frequently in the *S. cerevisiae* secretory pathway, as is the case of the chimeric fusions. Disregarding glycosylation and the linkers, the expected size of the UPO_AAO fusions was 97,000 Da, consistent with that of the deglycosylated fusion enzymes. Indeed, the wide smear at ∼200,000 Da produced by the different glycoforms in SDS-PAGE collapsed into tighter bands of ∼115,000 to ∼125,000 Da after treatment with PNGaseF, Figure 3B.

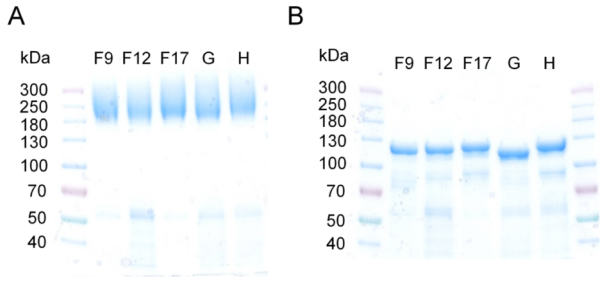

Figure 3. Molecular mass of UPO_AAO fusions. (A) Purified fusions and (B) fusions after treatment with PNGaseF resolved on 4−20% precast polyacrylamide gels.

The expression of the UPO_AAO fusion proteins was weaker than that of the individual secreted enzymes, on average 10- to 15-fold lower depending on the construct. However, the expression could be recovered by transferring the system from *S. cerevisiae* to the *P. pastoris* BSYBG11 strain and using the carbon source-repressed promoter P_{DF}.[52] P_{DF} permits methanol-independent protein expression, which may favor an alternative *P. pastoris* recombinant protein production because of the toxicity and flammability of methanol. To benchmark the *S. cerevisiae* and *P. pastoris* production systems, the H enzyme fusion was cloned in the methanol-free *P. pastoris* strain, produced and purified. In contrast to the *S. cerevisiae* variant, the *P. pastoris* variant yielded a ∼140,000 Da band that was reduced to a ∼125,000 Da species by PNGaseF, highlighting its milder glycosylation (roughly 10%) as would be expected in *P. pastoris*, Figure S2. In the flask, the production yield increased from 0.22 mg L^{-1} in *S. cerevisiae* to 7 mg L^{-1} in *P. pastoris*, a 32-fold improvement. This value will certainly increase when the strain is fermented in a fed-batch bioreactor because of the higher cell densities obtained in this format: ∼100 g of dry biomass L^{-1} in the bioreactor *versus* ∼10 g of dry biomass L^{-1} in flask production.[34,39]

We measured the steady kinetic parameters of purified UPO_AAO fusions and the individual secreted enzymes. Compared with AAO alone, the kinetics of the AAO partner were mostly conserved in all the fusions, while the catalytic efficiency of the UPO partner was reduced, with a 1.3- to 4-fold decrease in their activity relative to the individual secreted UPO, an effect that could be related to the strong hyperglycosylation shown in all the fusions, Table 3 and Figure 3. Moreover, kinetic constants slightly varied among the different fusions, as a consequence of the distinct composition and length of the linkers, which may affect the orientation between enzyme partners.

Production of Dextrorphan, an HDM from Dextromethorphan. The fusions were tested in a practical case, the synthesis of dextrorphan, a true HDM of the antitussive drug dextromethorphan. In this cascade reaction, primary aromatic alcohols were used as the substrates of the AAO partner in the fusion, as depicted in Scheme 1.

Several aromatic alcohols that are substrates of AAO may be also susceptible of transformation by UPO, which could lead to the imbalance of the cascade reaction. Accordingly, to rule out unwanted interactions between the aromatic alcohol and the UPO partner, while balancing the stoichiometric supply of H_2O_2, the following alcohols were tested: 4-fluorobenzyl alcohol (**2a**), 3-chlorobenzyl alcohol (**2b**), 4-chlorobenzyl alcohol (**2c**), 3-methoxybenzyl alcohol (**2d**), 4-methoxybenzyl alcohol (**2e**), and 3-hydroxy-4-methoxybenzyl alcohol (**2f**). The highest conversion was obtained when using the **2a**, **2d**, and **2e**, giving rise to total turnover numbers (TTNs, reported as μmol dextrorphan/μmol fusion enzyme) of up to ∼40,000 without further optimization, Figure 4A.

In previous studies, the catalytic efficiencies of recombinant AAO with these aromatic alcohols were reported as 59 and 65

https://dx.doi.org/10.1021/acscatal.0c03029
ACS Catal. 2020, 10, 13524−13534

Table 3. Kinetic Parameters of UPO_AAO Fusions and the Individual Enzymes[a]

substrate	kinetic constants	F9	F12	F17	G	H	AAO	UPO
4-methoxybenzyl alcohol (**2e**)	K_m (μM)	28 ± 0.4	38.2 ± 6	20.4 ± 3	21.4 ± 5.1	21.5 ± 3.2	23 ± 2	n.d
	k_{cat} (s^{-1})	30 ± 1	29 ± 1	44 ± 1	30 ± 2	34 ± 1	41 ± 1	n.d
	k_{cat}/K_m (mM^{-1} s^{-1})	1061	747	2183	1383	1568	1782	n.d
ABTS	K_m (μM)	733 ± 85	1375 ± 239	1204 ± 123	778 ± 119	667 ± 82		568 ± 91
	k_{cat} (s^{-1})	133 ± 6.5	209 ± 20	376 ± 20	250 ± 17	213 ± 11		365 ± 23
	k_{cat}/K_m (mM^{-1} s^{-1})	182	152	313	321	319		642

[a]The 4-methoxybenzyl (**2e**) kinetic constants for free AAO and AAO fusion partners were performed in 100 mM phosphate buffer with pH 6.0 at 25 °C. The ABTS kinetic constants for free UPO and UPO fusion partners were performed in 100 mM citrate phosphate buffer with pH 4.0 at 25 °C in the presence of 2 mM H_2O_2 (see the Materials and Methods section for details). All reactions were performed in triplicate. n.d. not determined.

Scheme 1. Cascade Reaction for the Synthesis of Dextrorphan[a]

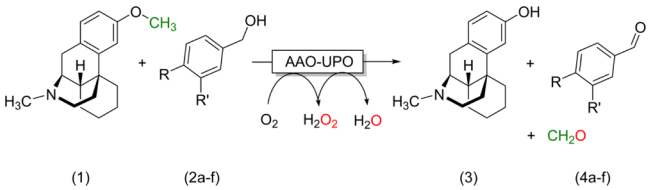

	2a/4a	2b/4b	2c/4c	2d/4d	2e/4e	2f/4f
R	F	H	Cl	H	OCH_3	OCH_3
R'	H	Cl	H	OCH_3	H	OH

[a]Dextromethorphan (**1**) is transformed by the AAO_UPO fusion into dextrorphan (**3**) through a cascade reaction; an aromatic alcohol (**2a–f**) is oxidized by the AAO partner into the corresponding aldehyde (**4a–f**), generating one equivalent of H_2O_2; the latter is used by the UPO partner to transform (**1**) into (**3**) through O-Dealkylation, releasing formaldehyde as a byproduct.

s^{-1} mM^{-1} for **2a** and **2d**, respectively; 152, 203, and 398 s^{-1} mM^{-1} for **2f**, **2b**, and **2c**, respectively; and 5233 s^{-1} mM^{-1} for **2e**.[53] This data addresses that the activity of the fusion is not related to the alcohol preferences by the AAO partner; that is, regardless of using the best (**2e**) or the worst (**2a**) alcohol for AAO, similar TTNs with the fusion were achieved, Figure 4A (kinetic values with recombinant evolved AAO expressed in *S. cerevisiae* gave similar values, see Table 4). The fact that AAO shows catalytic efficiencies with differences of 2 orders of magnitude for the two best alcohols used in the cascade points the activity of UPO toward these aromatic alcohols as the key driver of the whole cascade reaction (*i.e.*, the lower the UPO activity against the aromatic alcohol, the higher the TTN with dextromethorphan). To confirm this hypothesis, we measured the kinetic values of the best (**2a**) and the worst (**2c**) alcohols of the cascade, as well as of dextromethorphan. Indeed, the higher affinity of **2c** for UPO's catalytic site when compared to dextromethorphan (with K_m values of 1670 ± 170 and 3554 ± 725 μM, respectively, Table 4) addresses **2c** as a strong competitor of dextromethorphan, which limits the performance of the fusion in the production of dextrorphan, Figure 4A. By contrast, with **2a**, it was not even possible to determine the kinetics because of the higher K_m, far beyond the water solubility of the substrate, and therefore becoming an ideal substrate to boost the cascade, Figure S3.

The UPO_AAO fusions were accordingly benchmarked with **2a** as the departure alcohol, with the H fusion producing ~2 mM of dextrorphan with a TTN of 48,300 after optimizing

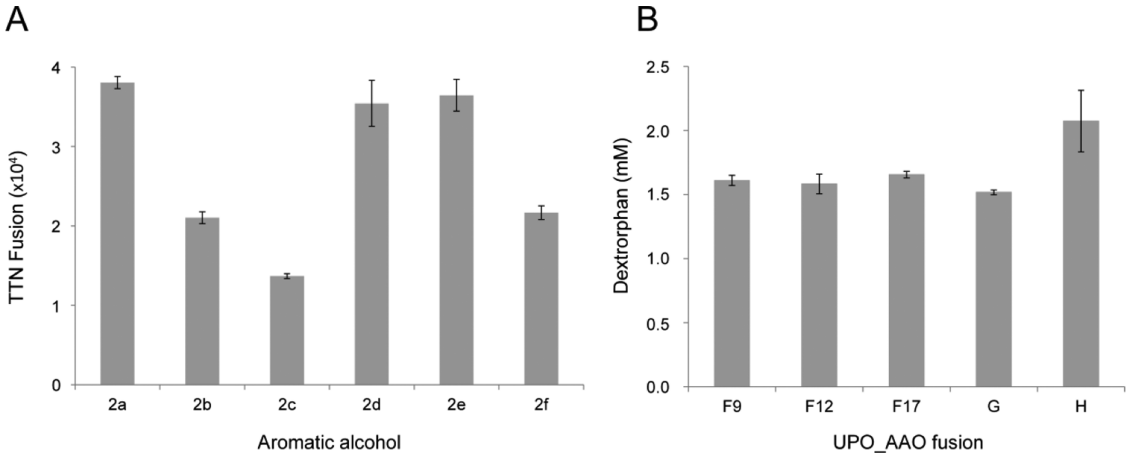

Figure 4. Aromatic alcohol selection and fusion enzyme performance in the production of dextrorphan. (A) TTNs for the transformation of dextromethorphan into dextrorphan. Reactions were performed in 1.5 mL GC vials in a final volume of 0.3 mL containing 10 mM of each aromatic alcohol, 0.04 μM of the H fusion (peroxygenase partner concentration measured with the CO difference spectrum), and 10 mM dextromethorphan hydrobromide in 100 mM potassium phosphate buffer at pH 7.0. (B) Comparison of the different UPO_AAO fusions with **2a** and dextromethorphan. The reactions were performed in 1.5 mL GC vials in a final volume of 0.3 mL containing 10 mM **2a**, 0.05 μM of each UPO_AAO fusion (a peroxygenase partner concentration measured with the CO difference spectrum), and 10 mM dextromethorphan hydrobromide in 100 mM potassium phosphate buffer at pH 7.0. All reactions were incubated for 24 h at 30 °C and at 600 rpm. The reactions were performed in duplicate at least and analyzed by GC-FID, as described in the Materials and Methods section.

https://dx.doi.org/10.1021/acscatal.0c03029
ACS Catal. 2020, 10, 13524−13534

Table 4. Kinetic Parameters of H and the Individual Enzymes with a Comparison between the Best (2a) and the Worst (2c) Alcohol for the Cascade[a]

substrate	kinetic constants	H	AAO	UPO
4-fluorobenzyl alcohol (**2a**)	K_m (μM)	630 ± 54	584 ± 19	n.m.
	k_{cat} (s^{-1})	25.7 ± 1.1	26.7 ± 0.4	n.m.
	k_{cat}/K_m (mM^{-1} s^{-1})	41	46	n.m.
4-chlorobenzyl alcohol (**2c**)	K_m (μM)	103 ± 4	104 ± 6	1670 ± 170
	k_{cat} (s^{-1})	28.1 ± 0.3	33.8 ± 0.5	339.2 ± 16.6
	k_{cat}/K_m (mM^{-1} s^{-1})	272	325	203
dextromethorphan	K_m (μM)	7387 ± 2807		3554 ± 725
	k_{cat} (s^{-1})	2298 ± 432		1395 ± 121
	k_{cat}/K_m (mM^{-1} s^{-1})	311		402

[a]4-Fluorobenzyl and 4-chlorobenzyl alcohol kinetic constants for free AAO and AAO fusion partners were estimated in 100 mM phosphate buffer with pH 6.0 at 25 °C. 4-Fluorobenzyl and 4-chlorobenzyl alcohol kinetic constants for free UPO were estimated in 100 mM citrate phosphate buffer with pH 6.0 at 25 °C in the presence of 2 mM H_2O_2. Dextromethorphan kinetic constants for free UPO and UPO fusion partners were estimated in 100 mM citrate phosphate buffer with pH 6.0 at 25 °C in the presence of 2 mM H_2O_2 and measured with the Purpald colorimetric assay (see the Materials and Methods section for details). All reactions were performed in triplicate. n.m: not measurable because of the high K_m value and the poor solubility of the substrate at concentrations over 20 mM (see Figure S3).

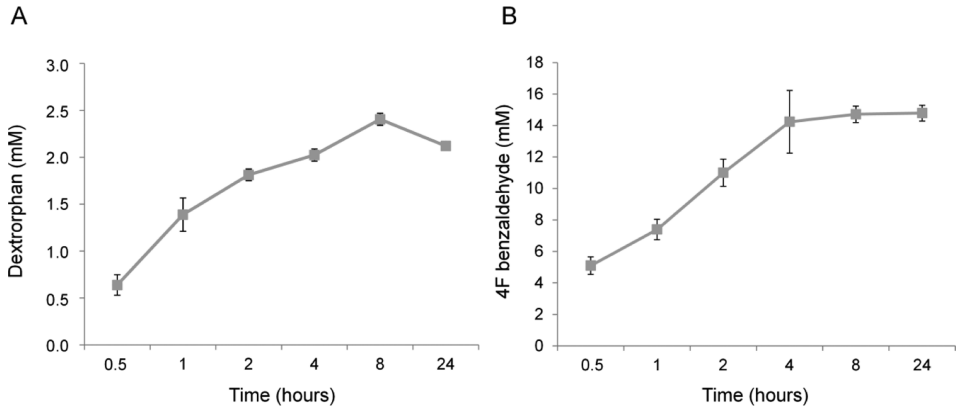

Figure 5. Time course of the fusion H reaction. (A) Dextrorphan production (UPO activity). (B) **2a** oxidation (AAO activity). The reactions were performed in 1.5 mL GC vials in a final volume of 0.3 mL containing 15 mM of **2a**, 0.1 μM of H (peroxygenase concentration measured with the CO difference spectrum), and 10 mM of dextromethorphan hydrobromide (**1**) in 100 mM potassium phosphate buffer at pH 7.0. Reactions were incubated at 30 °C and at 600 rpm in a ThermoMixer C and extracted with ethyl acetate at different time points to stop the reactions (0.5, 1, 2, 4, 8, and 24 h). All reactions were performed at least in duplicate.

the reaction conditions (see the Materials and Methods section for details), Figure 4B. To the best of our knowledge, this value is the highest TTN ever reported for the enzymatic synthesis of dextrorphan, followed far behind by the recently described sulfite oxidase-peroxygenase cascade system[9] with a TTN of 10,540 (*i.e.*, 4-fold less than the current chimeric fusion system). This difference is even more dramatic when compared to the performance of the UPO mutant without the H_2O_2 cascade, which only achieved 7500 TTN.[32] The performance of the H fusion was compared to that of the free UPO and AAO enzyme cocktail. After 15 min of reaction and applying equal equimolar enzyme concentrations in both the fusion and the free enzyme cocktail, the H fusion doubled the production of dextrorphan. After 45 min of reaction, a plateau was reached with TTNs of 32,100 and 21,200 for the H fusion and the enzyme cocktail, respectively, Figure S4. The differences observed between both systems seem to address a substrate channeling effect, minimizing the diffusion of H_2O_2 between the fusion partners and therefore becoming the main responsible for the improved performance of the fusion. Crystallization of the fusion along with computational ligand diffusion experiments could shed light into this matter.

To further characterize the enzymatic cascade of the H fusion, a time course reaction was performed, Figure 5. The yield of dextrorphan produced by the UPO partner remained linear during the first hour, slowing down to reach a maximum after 8 h, Figure 5A. Oxidation of **2a** to **4a** proceeded significantly faster than the coupled hydroxylation of **1** to **3**, Figure 5. Hence, *in situ* accumulation of H_2O_2 occurred, which most likely inactivated the UPO subunit of the fusion enzyme, thereby limiting its turnover number in dextrorphan synthesis to approximately 25,000. Because the K_m value for the benzyl alcohol substrate is in the millimolar range, we hypothesized that limiting the *in situ* concentration of **2a** (by using a syringe pump) may lead to a more balanced oxidase/peroxygenase activity. Indeed, using the fed-batch strategy with **2a** dosing rates of 0.5, 1, and 2 mM h^{-1} resulted in TTN for the dextrorphan synthesis of 62,145, 59,104, and 54,535, respectively, Figure S5. The benefits of controlling the alcohol dosing agrees well with previous studies on P450 $OleT_{JE}$ fused to an alditol oxidase.[54]

CONCLUSIONS

Advances in directed evolution in yeast and progress in the engineering of chimeric fusion proteins has allowed us to

https://dx.doi.org/10.1021/acscatal.0c03029
ACS Catal. 2020, 10, 13524−13534

design the first UPO_AAO fusion that could be employed in the synthesis of a range of pharmaceutical and chemical products. Indeed, the enzymatic production of HDMs is gaining momentum, with peroxygenases and P450 monooxygenases sharing the headlines in this important field of research.[4,55−59] Given the unique partnership between AAO and UPO, the fusion construct designed here could be further applied and evolved in the laboratory for more complex cascade reactions that harness the activity of both these enzymes, such as the six-electron oxidation of 5-hydroxymethyl furfural to furan-2,5-dicarboxylic acid, an attractive building block for renewable plastics (currently under study).[33,60] From a more general perspective, the directed evolution of the linker itself or of the whole system could enhance the activities of both partners, fine-tuning the generation of H_2O_2 in the context of a given biotransformation.

MATERIALS AND CULTURE MEDIA

Materials. Aromatic alcohols, Purpald, dextrorphan, and the yeast transformation kit were purchased from Sigma-Aldrich/Merck (Darmstadt, Germany). Dextromethorphan hydrobromide was purchased from Santa Cruz Biotechnology (CA, USA). The high-fidelity DNA polymerase iProof was acquired from Bio-Rad (CA, USA). The BamHI and XhoI restriction enzymes were purchased from New England Biolabs (MA, USA), and the protease-deficient *S. cerevisiae* strain BJ5465 was from LGCPromochem (Barcelona, Spain). *Escherichia coli* XL2-Blue competent cells were from Stratagene (CA, USA). *P. pastoris* strain BSYBG11 and plasmid pBSY5Z were kindly provided by Bisy (Graz, Austria). The Zymoprep Yeast Plasmid Miniprep kit was from Zymo Research (CA, USA). The NucleoSpin Plasmid kit and the NucleoSpin Gel and PCR Clean-up kit were purchased from Macherey-Nagel (Düren, Germany), H linker was synthesized at ATG/biosynthetics GmbH (Merzhausen, Germany), and the oligonucleotides were synthesized by IDT (IA, USA). All chemicals were of reagent-grade purity or of analytical standards.

Culture Media. The sterile liquid minimal medium contained 100 mL of 6.7% filtered yeast nitrogen base, 100 mL of 19.2 g L^{-1} filtered yeast synthetic dropout medium supplement without uracil, 100 mL of filtered 20% raffinose, 700 mL of ddH_2O, and 1 mL 25 g L^{-1} of filtered chloramphenicol. The SC dropout plates contained 100 mL of 6.7% filtered yeast nitrogen base, 100 mL of 19.2 g L^{-1} filtered yeast synthetic dropout medium supplement without uracil, 100 mL of 20% filtered glucose, 20 g of autoclaved bacto agar, 1 mL of 25 g L^{-1} filtered chloramphenicol, and 1000 mL of ddH_2O. The sterile expression medium contained 720 mL of autoclaved YP, 67 mL of 1 M filtered KH_2PO_4 pH 6.0 buffer, 111 mL of 20% filtered galactose, 22 mL of filtered $MgSO_4$ 0.1 M, 1 mL of 25 g L^{-1} filtered chloramphenicol, and 1000 mL of ddH_2O. The Luria broth (LB) medium contained 10 g of sodium chloride, 5 g of yeast extract, 10 g of peptone, 1 mL of ampicillin at 100 mg mL^{-1}, and 1000 mL of ddH_2O.

METHODS

Fusion Engineering. PCRs for creation of the linkers and fusions were carried out with the primers listed in Table S1. The PCR mixtures contained the following: PCR 1: 50 μL final volume, dimethyl sulfoxide (DMSO) (3%), primer XR (where X is the construction name) (0.5 μM), RMLN (0.5 μM), dNTPs (1 mM, 0.25 mM each), high-fidelity DNA polymerase iProof (0.02 U mL^{-1}), and the template SoLo (construction A, B, B′, E, F, G, H, I, J, K, and L) or FX9 (constructions C and D) (10 ng). PCR 2.1: for the case of constructions A, B, B′, C, and D, because of the length of the linker, an additional PCR had to be carried out: 50 μL final volume, DMSO (3%), primer XF1 (0.5 μM), RMLC (0.5 μM), dNTPs (1 mM, 0.25 mM each), high-fidelity DNA polymerase iProof (0.02 U mL^{-1}), and the template SoLo (constructions C and D) or FX9 (constructions A, B, and B′) (10 ng). PCR 2.2: PCR mixtures contained 50 μL final volume, DMSO (3%), primer XF1 (0.5 μM), RMLN (0.5 μM), dNTPs (1 mM, 0.25 mM each), high-fidelity DNA polymerase iProof (0.02 U mL^{-1}), and the template (fragment from PCR 2.1) (10 ng). PCR 3: constructions E, F, G, H, I, J, K, and L. PCR mixtures contained 50 μL final volume, DMSO (3%), primer XF1 (0.5 μM), RMLC (0.5 μM), dNTPs (1 mM, 0.25 mM each), high-fidelity DNA polymerase iProof (0.02 U mL^{-1}), and the template FX9 (10 ng). PCR linker: H linker was synthetized and extracted from commercial pUC18 with a PCR of 50 μL final volume, DMSO (3%), primer HF2 (0.5 μM), primer HR2 (0.5 μM), dNTPs (1 mM, 0.25 mM each), high-fidelity DNA polymerase iProof (0.02 U mL^{-1}), and the template (pUC18-Hlinker) (10 ng). All PCRs were carried out in a gradient thermocycler using the following parameters: 98 °C for 30 s (one cycle); 98 °C for 10 s, 45 °C for 30 s, and 72 °C for 120 s (28 cycles); and 72 °C for 10 min (one cycle). PCR products were loaded onto a preparative agarose gel and purified with the NucleoSpin Gel and PCR Clean-Up kit. The recovered DNA fragments were cloned under the control of the GAL1 promoter of the pJRoC30 expression shuttle vector, with the use of BamHI and XhoI to linearize the plasmid and to remove the parent gene. The linearized vector was loaded onto a preparative agarose gel and purified with the NucleoSpin Gel and PCR Clean-Up kit. The PCR products (200 ng each) were mixed with the linearized plasmid (100 ng) and transformed into *S. cerevisiae* for *in vivo* gene reassembly and cloning by IVOE,[61] Figure S1.

After selecting the best candidates for protein characterization, they were cloned with a His tag in the C-terminal of the fusion protein. For this purpose, two PCRs were performed, the first one being the template for the second one. The His tag coding sequence is underlined in each primer. PCR 1.His: 50 μL final volume, DMSO (3%), primer RHis1 (5′-CTAATGATGATGATGATGCTGATCAGCCTTGATAAGATCGGCT-3′) (0.5 μM), RMLN (0.5 μM), dNTPs (1 mM, 0.25 mM each), high-fidelity DNA polymerase iProof (0.02 U mL^{-1}), and the template (constructions F9, F12, F17, G, and H) (10 ng). PCR 2.His: 50 μL final volume, DMSO (3%), primer RHis2 (5′-CATAACTAATTACATGATGCGGCCCTCTAGATGCATGCTCGAGCGGCCGCCTAATGATGATGATGATGATGCTGATC-3′) (0.5 μM), RMLN (0.5 μM), dNTPs (1 mM, 0.25 mM each), high-fidelity DNA polymerase iProof (0.02 U mL^{-1}), and the template (PCR 1.His) (10 ng). PCRs were carried out in a gradient thermocycler using the following parameters: 98 °C for 30 s (1 cycle); 98 °C for 20 s, 45 °C (PCR 1.His) or 50 °C (PCR 2.His) for 30 s, and 72 °C for 120 s (30 cycles); and 72 °C for 20 min (1 cycle). PCR products were prepared and transformed as described before. The H construction was further cloned in *P. pastoris* BSYBG11 under the P_{DF} promoter with the same signal peptide used in *S. cerevisiae*. P_{DF} is an orthologous promoter of P_{DC}, *P. pastoris*

https://dx.doi.org/10.1021/acscatal.0c03029
ACS Catal. 2020, 10, 13524−13534

CAT1 promoter (PCAT1-500). Expression conditions were the ones described before with minor modifications.[52]

Activity Screening Assays. *ABTS/H_2O_2 Assay.* Aliquots of 20 μL of yeast supernatants were added to 180 μL of reaction mixture for ABTS screening containing 100 mM sodium citrate-phosphate at pH 4.0, 5 mM ABTS, and 2 mM H_2O_2. The plates were measured in kinetic or end point mode at 418 nm ($\varepsilon ABTS^{\bullet+}$ = 36,000 M^{-1} cm^{-1}) (SpectraMax Plus, Molecular Devices). The UPO activity is defined as the amount of enzyme that converts 1 μmol of ABTS to $ABTS^{\bullet+}$ per min under the reaction conditions.

4-Methoxybenzyl Alcohol/ABTS−HRP-Coupled Assay. Aliquots of 20 μL of yeast supernatants were added to 180 μL of HRP-ABTS reagent (final concentrations of HRP-ABTS reagent in the well: 1 mM 4-methoxybenzyl alcohol, 2.5 mM ABTS, and 1 μg of HRP mL^{-1} (horseradish peroxidase) in 100 mM phosphate buffer [pH 6.0]). The plates were incubated at room temperature and measured in kinetic or end point mode at 418 nm. The AAO activity is defined as the amount of enzyme that converts 1 μmol of alcohol to aldehyde with the stoichiometric formation of H_2O_2 per min under the reaction conditions.

4-Methoxybenzyl Alcohol/ABTS Assay. Aliquots of 20 μL of yeast supernatants were added to 180 μL of reaction mixture containing 100 mM sodium citrate-phosphate at pH 4.0, 5 mM ABTS, and 1 mM 4-methoxybenzyl alcohol. The plates were incubated at room temperature and measured in the end point mode at 418 nm.

Expression and Purification of Enzyme Fusions. *Expression in Microplate and Selection of the Constructs.* Individual clones were picked and cultured in sterile 96-well plates containing 50 μL of minimal medium (SC). In each plate, column 6 was inoculated with SoLo (UPO), column 7 with FX9 (AAO), and well H1 was not inoculated (culture media control). The plates were sealed to prevent evaporation and incubated at 30 °C, 225 rpm, and 80% relative humidity in a humidity shaker (Minitron-INFORS; Biogen, Spain). After 48 h, 150 μL of expression medium was added to each well, followed by culture for additional 48 h at 25 °C. The plates were centrifuged at 2000 rpm (at 4 °C), and finally, 20 μL portions of the supernatants were screened for activity with the AAO, UPO, and enzyme fusion mix assays. The plasmids from positive wells were recovered with the Zymoprep yeast plasmid miniprep kit I. Because the product of Zymoprep was impure and the DNA extracted was very low-concentrated, the shuttle vectors were transformed into supercompetent *E. coli* XL2-Blue cells and plated onto LB-ampicillin plates. Single colonies were selected to inoculate 5 mL of LB-ampicillin medium and incubated overnight at 37 °C and 225 rpm. The plasmids from the best mutants were extracted (NucleoSpin plasmid kit), sent for DNA sequencing (GATC Biotech-Eurofins, Luxembourg), and transformed into *S. cerevisiae* for flask production.

Large-Scale Production and Purification. Single colonies from the *S. cerevisiae* clones containing the constructs were picked from an SC dropout plate, inoculated in minimal medium (10 mL), and incubated for 48 h at 30 °C and 230 rpm. An aliquot of cells was removed and used to inoculate the minimal medium (100 mL) in a 500 mL shake flask (at OD_{600} ~ 0.25). The cells completed two growth phases (8 h) and then the expression medium (900 mL) was inoculated with the preculture (100 mL) (OD_{600} of 0.1). After incubating for 72 h at 25 °C and 150 rpm (maximal enzyme activity; OD_{600} = 25−30) in 2500 mL baffled Ultra Yield flasks (Thomson Instruments Inc., CA, USA), the cells were recovered by centrifugation at 8000 rpm (at 4 °C) and the supernatant was double-filtered (using both glass membrane and a nitrocellulose membrane of 0.45 μm pore size). Enzyme fusions were purified by immobilized metal-ion affinity chromatography (IMAC) using HisTrap FF columns (GE Healthcare, ON, Canada) coupled to an ÄKTA purifier system. Binding buffer contained 20 mM bis-Tris at pH 7.4, 250 mM NaCl, 10 mM imidazole and elution buffer, 20 mM bis-Tris at pH 7.4, 250 mM NaCl, and 200 mM imidazole. IMAC-purified enzyme fusions were dialyzed for desalting and further purification by size exclusion chromatography (SEC) using a Superdex 75 Increase 10/300 GL SEC column (GE Healthcare) in a running buffer (50 mM potassium phosphate at pH 7, 150 mM NaCl) at 0.8 mL min^{-1}. Fractions presenting both UPO and AAO activities were pooled, concentrated, and dialyzed against stability buffer (20 mM potassium phosphate at pH 7), resulting in pure orange proteins (this coloration is due to the presence of heme group -red- and FAD -yellow- inside the protein). Samples were loaded onto 4−20% precast polyacrylamide gel under denaturing conditions (Bio-Rad). Enzymes were deglycosylated with PNGase F (New England Biolabs, MA, USA) following the commercial protocol under denaturing conditions. The concentration of UPO for TTN calculations was determined using the CO (carbon monoxide) difference spectrum. It was performed at 25 °C using Tris-HCl buffer (20 mM, pH 7.0) and sodium dithionite (50 mM). The samples were bubbled with CO for 60 s (1−2 bubbles per sec). The CO difference spectra were recorded between 400 and 500 nm. From the absorbance difference between 445 and 490 nm, the peroxygenase concentration can be calculated using an extinction coefficient of $\varepsilon_{445-490}$ = 107 mM^{-1} cm^{-1}. FX9 (AAO) and SoLo (UPO) were produced and purified as described elsewhere.[31,34] Concentrations of the enzymes were determined with Bio-Rad protein reagent and bovine serum albumin as a standard.

Kinetic Characterization. ABTS kinetic constants were estimated at 25 °C in 100 mM sodium phosphate/citrate buffer at pH 4.0 containing 2 mM H_2O_2. 4-Methoxybenzyl alcohol (**2e**), 4-chlorobenzyl alcohol (**2c**), and 4-fluorobenzyl alcohol (**2a**) kinetics were measured in 100 mM potassium phosphate buffer at pH 6.0 for AAO and UPO_AAO and adding 2 mM H_2O_2 for UPO. The reactions were performed in triplicate, and substrate oxidations were followed through spectrophotometric changes (ε_{418} $ABTS^{\bullet+}$ = 36,000 M^{-1} cm^{-1}; ε_{285} 4-methoxybenzaldehyde = 16,950 M^{-1} cm^{-1}; ε_{252} 4-fluorobenzaldehyde = 13,700 M^{-1} cm^{-1}; and ε_{260} 4-chlorobenzaldehyde = 15,862 M^{-1} cm^{-1}).[53] Dextromethorphan kinetics with SoLo and H enzyme fusions were carried out at 25 °C in 100 mM potassium phosphate buffer at pH 6.0 containing 2 mM H_2O_2 and 0.5−10 mM dextromethorphan. Dextromethorphan kinetics were estimated with the help of Purpald reagent (it reacts with formaldehyde—a byproduct of dextromethorphan demethylation—giving a purple color measurable at 550 nm). After 40−480 s, depending on the dextromethorphan concentration, aliquots of 10 μL were withdrawn and mixed with 140 μL of ddH_2O. Afterward, 50 μL of 100 mM Purpald dissolved in 2 N NaOH was added and mixed by stopping the reaction for 2 min. Absorbance was measured at 550 nm. Formaldehyde concentration determination was evaluated with a calibration curve, Figure S6. To calculate the K_m and k_{cat} values, the average V_{max} was represented against substrate concentration and fitted to a

https://dx.doi.org/10.1021/acscatal.0c03029
ACS Catal. 2020, 10, 13524−13534

single rectangular hyperbola function with SigmaPlot 10.0, where parameter a was equal to k_{cat} and parameter b was equal to K_m.

Evaluation of the Enzyme Fusion System. T_{50} values were determined as described elsewhere.[31] Dextrorphan synthesis was determined using a Shimadzu GC-2010 Plus gas chromatograph with an AOC-20i Auto injector with an FID detector (Shimadzu, Japan) using nitrogen as the carrier gas with a previously described method.[9] The reactions were performed in GC vials of 1.5 mL in a final volume of 0.3 mL. For the evaluation of the performance of different alcohols within the cascade, the reactions contained 10 mM of each primary alcohol (**2a**−**f**), 0.04 μM of H (peroxygenase concentration measured with the CO difference spectrum) and 10 mM of dextromethorphan hydrobromide in 100 mM potassium phosphate buffer at pH 7.0 were carried out. Comparison of enzyme fusions was performed with 10 mM of **2a**, 0.05 μM of each enzyme fusion, and 10 mM of dextromethorphan hydrobromide in 100 mM potassium phosphate buffer at pH 7.0. Optimized reaction conditions were achieved with 2 mM of **2a**, 0.04 μM of enzyme fusion H (peroxygenase concentration measured with the CO difference spectrum), and 10 mM of dextromethorphan hydrobromide in 100 mM potassium phosphate buffer at pH 7.0. Concerning alcohol feeding experiments, initial reaction mixtures contained 0.04 μM of H fusion and 10 mM of dextromethorphan hydrobromide in 100 mM potassium phosphate buffer at pH 7.0. **2a** was added inside the vial with a tubing connected to a syringe pump (1 μL h^{-1}) at three different rates (0.5, 1, and 2 mM h^{-1}), achieved with a different stock concentration of alcohol inside the syringes, Figure S5. All reactions were incubated for 24 h at 30 °C and 600 rpm in a ThermoMixer C and they were performed at least by duplicate. Time course reactions contained 15 mM of **2a**, 0.1 μM of H fusion, and 10 mM of dextromethorphan hydrobromide in 100 mM potassium phosphate buffer at pH 7.0. The reaction was extracted with ethyl acetate at different time points (0.5, 1, 2, 4, 8, and 24 h).

H enzyme fusion performance compared to the use of both free enzymes separately (FX9 and SoLo) was evaluated in triplicate in GC vials of 1.5 mL in a final volume of 0.2 mL containing 10 mM of **2a**, 10 mM of dextromethorphan hydrobromide in 100 mM potassium phosphate buffer at pH 6.0 and 0.1 μM of H fusion (peroxygenase concentration measured with the CO difference spectrum) (H fusion UPO_AAO) or 0.1 μM of FX9 (AAO) and 0.1 μM of SoLo (UPO) (UPO + AAO). The reactions were incubated for 1 h at 30 °C and 600 rpm in a ThermoMixer C. Aliquots of 7.5 μL were withdrawn from each vial at time points 15, 30, 45, and 60 min for product determination using the Purpald assay. The aliquots were added to 142.5 μL of ddH_2O (1/20 dilution) and further mixed for 2 min with 50 μL of 100 mM Purpald dissolved in 2N NaOH and immediately measured at 550 nm as described before.

■ ASSOCIATED CONTENT

Supporting Information

The Supporting Information is available free of charge at https://pubs.acs.org/doi/10.1021/acscatal.0c03029.

Sequences of primers and amino acids of the linkers; cloning strategy for the creation of the different linkers based on homologous DNA recombination *in vivo*; SDS-PAGE; kinetic plots of UPO with 4-fluorobenzyl alcohol and 4-chlorobenzyl alcohol; comparison between fused and nonfused enzymes; reaction setup for dextrorphan production; and Purpald assay and calibration curve (PDF)

■ AUTHOR INFORMATION

Corresponding Author

Miguel Alcalde − *Department of Biocatalysis, Institute of Catalysis, CSIC, 28049 Madrid, Spain; EvoEnzyme S.L., 28049 Madrid, Spain;* orcid.org/0000-0001-6780-7616; Email: malcalde@icp.csic.es

Authors

Patricia Gomez de Santos − *Department of Biocatalysis, Institute of Catalysis, CSIC, 28049 Madrid, Spain*

Sofia Lazaro − *Department of Biocatalysis, Institute of Catalysis, CSIC, 28049 Madrid, Spain*

Javier Viña-Gonzalez − *Department of Biocatalysis, Institute of Catalysis, CSIC, 28049 Madrid, Spain; EvoEnzyme S.L., 28049 Madrid, Spain*

Manh Dat Hoang − *Department of Biocatalysis, Institute of Catalysis, CSIC, 28049 Madrid, Spain; Institute of Biochemical Engineering, Technical University of Munich, 85748 Garching, Germany*

Israel Sánchez-Moreno − *Department of Biocatalysis, Institute of Catalysis, CSIC, 28049 Madrid, Spain*

Anton Glieder − *Institute of Molecular Biotechnology, Graz University of Technology, 8010 Graz, Austria; Bisy e.U., 8200 Hofstaetten a. d. Raab, Austria*

Frank Hollmann − *Department of Biotechnology, Delft University of Technology, 2629HZ Delft, The Netherlands;* orcid.org/0000-0003-4821-756X

Complete contact information is available at: https://pubs.acs.org/10.1021/acscatal.0c03029

Notes

The authors declare the following competing financial interest(s): The UPO variant used in the current study is protected by a CSIC patent WO/2017/081355 (licensed in exclusivity to EvoEnzyme S.L). Bisy E.U. declares interest in the commercialization of the new de-repressed promoters used in this study.

■ ACKNOWLEDGMENTS

This work was supported by the Comunidad de Madrid Synergy CAM project Y2018/BIO-4738-EVOCHIMERA-CM, the Spanish Government Projects BIO2016-79106-R-Lignolution, PID2019-106166RB-100-OXYWAVE, and the CSIC project PIE-201580E042. P.G.d.S. is grateful to the Ministry of Science, Innovation and Universities (Spain), for her FPI contract (BES-2017-080040).

■ REFERENCES

(1) Molina-Espeja, P.; Gomez de Santos, P.; Alcalde, M. Directed Evolution of Unspecific Peroxygenase. In *Directed Enzyme Evolution: Advances and Applications*; Alcalde, M., Ed.; Springer International Publishing: Cham, 2017; pp 127−143.

(2) Hofrichter, M.; Ullrich, R. Oxidations Catalyzed by Fungal Peroxygenases. *Curr. Opin. Chem. Biol.* **2014**, *19*, 116−125.

(3) Hofrichter, M.; Kellner, H.; Herzog, R.; Karich, A.; Liers, C.; Scheibner, K.; Kimani, V. W.; Ullrich, R. Fungal Peroxygenases: A Phylogenetically Old Superfamily of Heme Enzymes with Promiscuity

for Oxygen Transfer Reactions. In *Grand Challenges in Fungal Biotechnology*; Nevalainen, H., Ed.; Springer International Publishing: Cham, 2020; pp 369−403.
(4) Kiebist, J.; Hofrichter, M.; Zuhse, R.; Scheibner, K. Oxyfunctionalization of Pharmaceuticals by Fungal Peroxygenases. In *Pan Standford Series on Biocatalysis*; Grundwal, P., Ed.; Pan Stanford Publishing, 2019; Vol. 4, pp 643−680.
(5) Wang, Y.; Lan, D.; Durrani, R.; Hollmann, F. Peroxygenases En Route to Becoming Dream Catalysts. What Are the Opportunities and Challenges? *Curr. Opin. Chem. Biol.* **2017**, *37*, 1−9.
(6) Bormann, S.; Gomez Baraibar, A.; Ni, Y.; Holtmann, D.; Hollmann, F. Specific Oxyfunctionalisations Catalysed by Peroxygenases: Opportunities, Challenges and Solutions. *Catal. Sci. Technol.* **2015**, *5*, 2038−2052.
(7) Fernández-Fueyo, E.; Ni, Y.; Gomez Baraibar, A.; Alcalde, M.; van Langen, L. M.; Hollmann, F. Towards Preparative Peroxygenase-Catalyzed Oxyfunctionalization Reactions in Organic Media. *J. Mol. Catal. B: Enzym.* **2016**, *134*, 347−352.
(8) Zhang, W.; Burek, B. O.; Fernández-Fueyo, E.; Alcalde, M.; Bloh, J. Z.; Hollmann, F. Selective Activation of C−H Bonds in a Cascade Process Combining Photochemistry and Biocatalysis. *Angew. Chem., Int. Ed.* **2017**, *56*, 15451−15455.
(9) van Schie, M. M. C. H.; Kaczmarek, A. T.; Tieves, F.; Gomez de Santos, P.; Paul, C. E.; Arends, I. W. C. E.; Alcalde, M.; Schwarz, G.; Hollmann, F. Selective Oxyfunctionalisation Reactions Driven by Sulfite Oxidase-Catalysed In Situ Generation of H 2 O 2. *ChemCatChem* **2020**, *12*, 3186−3189.
(10) Willot, S. J. P.; Hoang, M. D.; Paul, C. E.; Alcalde, M.; Arends, I. W. C. E.; Bommarius, A. S.; Bommarius, B.; Hollmann, F. FOx News: Towards Methanol-driven Biocatalytic Oxyfunctionalisation Reactions. *ChemCatChem* **2020**, *12*, 2713−2716.
(11) Yoon, J.; Kim, J.; Tieves, F.; Zhang, W.; Alcalde, M.; Hollmann, F.; Park, C. B. Piezobiocatalysis: Ultrasound-Driven Enzymatic Oxyfunctionalization of C-H Bonds. *ACS Catal.* **2020**, *10*, 5236−5242.
(12) Hobisch, M.; van Schie, M. M. C. H.; Kim, J.; Andersen, K. R.; Alcalde, M.; Kourist, R.; Park, C. B.; Hollmann, F.; Kara, S. Solvent-Free Photobiocatalytic Hydroxylation of Cyclohexane. *ChemCatChem* **2020**, *12*, 3956.
(13) Zhang, W.; Fernández-Fueyo, E.; Ni, Y.; van Schie, M. M. C. H.; Gacs, J.; Renirie, R.; Wever, R.; Mutti, F. G.; Rother, D.; Alcalde, M.; Hollmann, F. Selective Aerobic Oxidation Reactions Using a Combination of Photocatalytic Water Oxidation and Enzymatic Oxyfunctionalisations. *Nat. Catal.* **2018**, *1*, 55−62.
(14) Tieves, F.; Willot, S. J. P.; van Schie, M. M. C. H.; Rauch, M. C. R.; Younes, S. H. H.; Zhang, W.; Dong, J.; Gomez de Santos, P.; Robbins, J. M.; Bommarius, B.; Alcalde, M.; Bommarius, A. S.; Hollmann, F. Formate Oxidase (FOx) from Aspergillus Oryzae: One Catalyst Enables Diverse H2O2-Dependent Biocatalytic Oxidation Reactions. *Angew. Chem., Int. Ed.* **2019**, *58*, 7873−7877.
(15) Willot, S. J.P.; Fernández-Fueyo, E.; Tieves, F.; Pesic, M.; Alcalde, M.; Arends, I. W. C. E.; Park, C. B.; Hollmann, F. Expanding the Spectrum of Light-Driven Peroxygenase Reactions. *ACS Catal.* **2019**, *9*, 890−894.
(16) Burek, B. O.; de Boer, S. R.; Tieves, F.; Zhang, W.; van Schie, M. M. C. H.; Bormann, S.; Alcalde, M.; Holtmann, D.; Hollmann, F.; Bahnemann, D. W.; Bloh, J. Z. Photoenzymatic Hydroxylation of Ethylbenzene Catalyzed by Unspecific Peroxygenase: Origin of Enzyme Inactivation and the Impact of Light Intensity and Temperature. *ChemCatChem* **2019**, *11*, 3093−3100.
(17) van Schie, M. M. C. H.; Zhang, W.; Tieves, F.; Choi, D. S.; Park, C. B.; Burek, B. O.; Bloh, J. Z.; Arends, I. W. C. E.; Paul, C. E.; Alcalde, M.; Hollmann, F. Cascading G-C3N4 and Peroxygenases for Selective Oxyfunctionalization Reactions. *ACS Catal.* **2019**, *9*, 7409−7417.
(18) Freakley, S. J.; Kochius, S.; van Marwijk, J.; Fenner, C.; Lewis, R. J.; Baldenius, K.; Marais, S. S.; Opperman, D. J.; Harrison, S. T. L.; Alcalde, M.; Smit, M. S.; Hutchings, G. J. A Chemo-Enzymatic Oxidation Cascade to Activate C−H Bonds with in Situ Generated H2O2. *Nat. Commun.* **2019**, *10*, 4178.
(19) Li, Y.; Ma, Y.; Li, P.; Zhang, X.; Ribitsch, D.; Alcalde, M.; Hollmann, F.; Wang, Y. Enantioselective Sulfoxidation of Thioanisole by Cascading a Choline Oxidase and a Peroxygenase in the Presence of Natural Deep Eutectic Solvents. *Chempluschem* **2020**, *85*, 254−257.
(20) Yayci, A.; Baraibar, Á. G.; Krewing, M.; Fueyo, E. F.; Hollmann, F.; Alcalde, M.; Kourist, R.; Bandow, J. E. Plasma-Driven in Situ Production of Hydrogen Peroxide for Biocatalysis. *ChemSusChem* **2020**, *13*, 2072−2079.
(21) Aalbers, F. S.; Fraaije, M. W. Enzyme Fusions in Biocatalysis: Coupling Reactions by Pairing Enzymes. *ChemBioChem* **2019**, *20*, 20−28.
(22) Meinhold, P.; Peters, M. W.; Hartwick, A.; Hernandez, A. R.; Arnold, F. H. Engineering Cytochrome P450 BM3 for Terminal Alkane Hydroxylation. *Adv. Synth. Catal.* **2006**, *348*, 763−772.
(23) Colpa, D. I.; Lončar, N.; Schmidt, M.; Fraaije, M. W. Creating Oxidase-Peroxidase Fusion Enzymes as a Toolbox for Cascade Reactions. *Chembiochem* **2017**, *18*, 2226−2230.
(24) Hernández-Ortega, A.; Ferreira, P.; Martínez, A. T. Fungal Aryl-Alcohol Oxidase: A Peroxide-Producing Flavoenzyme Involved in Lignin Degradation. *Appl. Microbiol. Biotechnol.* **2012**, *93*, 1395−1410.
(25) Alcalde, M. Engineering the Ligninolytic Enzyme Consortium. *Trends Biotechnol.* **2015**, *33*, 155−162.
(26) Ruiz-Dueñas, F. J.; Martínez, Á. T. Microbial Degradation of Lignin: How a Bulky Recalcitrant Polymer Is Efficiently Recycled in Nature and How We Can Take Advantage of This. *Microb. Biotechnol.* **2009**, *2*, 164−177.
(27) Martínez, A. T.; Ruiz-Dueñas, F. J.; Camarero, S.; Serrano, A.; Linde, D.; Lund, H.; Vind, J.; Tovborg, M.; Herold-Majumdar, O. M.; Hofrichter, M.; Liers, C.; Ullrich, R.; Scheibner, K.; Sannia, G.; Piscitelli, A.; Pezzella, C.; Sener, M. E.; Kılıç, S.; van Berkel, W. J. H.; Guallar, V.; Lucas, M. F.; Zuhse, R.; Ludwig, R.; Hollmann, F.; Fernández-Fueyo, E.; Record, E.; Faulds, C. B.; Tortajada, M.; Winckelmann, I.; Rasmussen, J.-A.; Gelo-Pujic, M.; Gutiérrez, A.; del Río, J. C.; Rencoret, J.; Alcalde, M. Oxidoreductases on Their Way to Industrial Biotransformations. *Biotechnol. Adv.* **2017**, *35*, 815−831.
(28) Ruiz-Dueñas, F. J.; Ferreira, P.; Martínez, M. J.; Martínez, A. T. Vitro Activation, Purification, and Characterization of Escherichia Coli Expressed Aryl-Alcohol Oxidase, a Unique H2O2-Producing Enzyme. *Protein Expression Purif.* **2006**, *45*, 191−199.
(29) Linde, D.; Olmedo, A.; González-Benjumea, A.; Estévez, M.; Renau-Mínguez, C.; Carro, J.; Fernández-Fueyo, E.; Gutiérrez, A.; Martínez, A. T. Two New Unspecific Peroxygenases from Heterologous Expression of Fungal Genes in Escherichia Coli. *Appl. Environ. Microbiol.* **2020**, *86*, e02899−19.
(30) Carro, J.; González-Benjumea, A.; Fernández-Fueyo, E.; Aranda, C.; Guallar, V.; Gutiérrez, A.; Martínez, A. T. Modulating Fatty Acid Epoxidation vs Hydroxylation in a Fungal Peroxygenase. *ACS Catal.* **2019**, *9*, 6234−6242.
(31) Gomez de Santos, P.; Cañellas, M.; Tieves, F.; Younes, S. H. H.; Molina-Espeja, P.; Hofrichter, M.; Hollmann, F.; Guallar, V.; Alcalde, M. Selective Synthesis of the Human Drug Metabolite 5′-Hydroxypropranolol by an Evolved Self-Sufficient Peroxygenase. *ACS Catal.* **2018**, *8*, 4789−4799.
(32) Gomez de Santos, P.; Cervantes, F. V.; Tieves, F.; Plou, F. J.; Hollmann, F.; Alcalde, M. Benchmarking of Laboratory Evolved Unspecific Peroxygenases for the Synthesis of Human Drug Metabolites. *Tetrahedron* **2019**, *75*, 1827−1831.
(33) Viña-Gonzalez, J.; Martinez, A. T.; Guallar, V.; Alcalde, M. Sequential Oxidation of 5-Hydroxymethylfurfural to Furan-2,5-Dicarboxylic Acid by an Evolved Aryl-Alcohol Oxidase. *Biochim. Biophys. Acta, Proteins Proteomics* **2020**, *1868*, 140293.
(34) Viña-Gonzalez, J.; Elbl, K.; Ponte, X.; Valero, F.; Alcalde, M. Functional Expression of Aryl-Alcohol Oxidase in Saccharomyces Cerevisiae and Pichia Pastoris by Directed Evolution. *Biotechnol. Bioeng.* **2018**, *115*, 1666−1674.

(35) Martin-Diaz, J.; Paret, C.; García-Ruiz, E.; Molina-Espeja, P.; Alcalde, M. Shuffling the Neutral Drift of Unspecific Peroxygenase in Saccharomyces Cerevisiae. *Appl. Environ. Microbiol.* **2018**, *84*, e00808−18.
(36) Mate, D. M.; Palomino, M. A.; Molina-Espeja, P.; Martin-Diaz, J.; Alcalde, M. Modification of the Peroxygenative:Peroxidative Activity Ratio in the Unspecific Peroxygenase from Agrocybe Aegerita by Structure-Guided Evolution. *Protein Eng., Des. Sel.* **2017**, *30*, 191−198.
(37) Molina-Espeja, P.; Garcia-Ruiz, E.; Gonzalez-Perez, D.; Ullrich, R.; Hofrichter, M.; Alcalde, M. Directed Evolution of Unspecific Peroxygenase from Agrocybe Aegerita. *Appl. Environ. Microbiol.* **2014**, *80*, 3496−3507.
(38) Molina-Espeja, P.; Cañellas, M.; Plou, F. J.; Hofrichter, M.; Lucas, F.; Guallar, V.; Alcalde, M. Synthesis of 1-Naphthol by a Natural Peroxygenase Engineered by Directed Evolution. *ChemBioChem* **2016**, *17*, 341−349.
(39) Molina-Espeja, P.; Ma, S.; Mate, D. M.; Ludwig, R.; Alcalde, M. Tandem-Yeast Expression System for Engineering and Producing Unspecific Peroxygenase. *Enzyme Microb. Technol.* **2015**, *73*−*74*, 29−33.
(40) Viña-Gonzalez, J.; Gonzalez-Perez, D.; Ferreira, P.; Martinez, A. T.; Alcalde, M. Focused Directed Evolution of Aryl-Alcohol Oxidase in Saccharomyces Cerevisiae by Using Chimeric Signal Peptides. *Appl. Environ. Microbiol.* **2015**, *81*, 6451−6462.
(41) Viña-Gonzalez, J.; Jimenez-Lalana, D.; Sancho, F.; Serrano, A.; Martinez, A. T.; Guallar, V.; Alcalde, M. Structure-Guided Evolution of Aryl Alcohol Oxidase from Pleurotus Eryngii for the Selective Oxidation of Secondary Benzyl Alcohols. *Adv. Synth. Catal.* **2019**, *361*, 2514−2525.
(42) Serrano, A.; Sancho, F.; Viña-González, J.; Carro, J.; Alcalde, M.; Guallar, V.; Martínez, A. T. Switching the Substrate Preference of Fungal Aryl-Alcohol Oxidase: Towards Stereoselective Oxidation of Secondary Benzyl Alcohols. *Catal. Sci. Technol.* **2019**, *9*, 833−841.
(43) Molina-Espeja, P.; Plou, F. J.; Alcalde, M.; Gomez de Santos, P. Mutants of Unspecific Peroxygenase with High Monooxygenase Activity and Uses Thereof. WO 2017081355 A1, 2016.
(44) Zhao, H. L.; Yao, X. Q.; Xue, C.; Wang, Y.; Xiong, X. H.; Liu, Z. M. Increasing the Homogeneity, Stability and Activity of Human Serum Albumin and Interferon-A2b Fusion Protein by Linker Engineering. *Protein Expression Purif.* **2008**, *61*, 73−77.
(45) Amet, N.; Lee, H.-F.; Shen, W.-C. Insertion of the Designed Helical Linker Led to Increased Expression of Tf-Based Fusion Proteins. *Pharm. Res.* **2008**, *26*, 523.
(46) Chen, X.; Zaro, J. L.; Shen, W.-C. Fusion Protein Linkers: Property, Design and Functionality. *Adv. Drug Delivery Rev.* **2013**, *65*, 1357−1369.
(47) Fernández, I. S.; Ruíz-Dueñas, F. J.; Santillana, E.; Ferreira, P.; Martínez, M. J.; Martínez, Á. T.; Romero, A. Novel Structural Features in the GMC Family of Oxidoreductases Revealed by the Crystal Structure of Fungal Aryl-Alcohol Oxidase. *Acta Crystallogr., Sect. D: Biol. Crystallogr.* **2009**, *65*, 1196−1205.
(48) Romanos, M. A.; Scorer, C. A.; Clare, J. J. Foreign Gene Expression in Yeast: A Review. *Yeast* **1992**, *8*, 423−488.
(49) Deng, Y.; Sun, M.; Xu, S.; Zhou, J. Enhanced (S)-Linalool Production by Fusion Expression of Farnesyl Diphosphate Synthase and Linalool Synthase in Saccharomyces Cerevisiae. *J. Appl. Microbiol.* **2016**, *121*, 187−195.
(50) Gustavsson, M.; Lehtiö, J.; Denman, S.; Teeri, T. T.; Hult, K.; Martinelle, M. Stable Linker Peptides for a Cellulose-Binding Domain−Lipase Fusion Protein Expressed in Pichia Pastoris. *Protein Eng., Des. Sel.* **2001**, *14*, 711−715.
(51) George, R. A.; Heringa, J. An Analysis of Protein Domain Linkers: Their Classification and Role in Protein Folding. *Protein Eng., Des. Sel.* **2002**, *15*, 871−879.
(52) Fischer, J. E.; Hatzl, A.-M.; Weninger, A.; Schmid, C.; Glieder, A. Methanol Independent Expression by Pichia Pastoris Employing De-Repression Technologies. *J. Visualized Exp.* **2019**, *143*, No. e58589.
(53) Ferreira, P.; Medina, M.; Guillén, F.; Martínez, M. J.; Van Berkel, W. J. H.; Martínez, Á. T. Spectral and Catalytic Properties of Aryl-Alcohol Oxidase, a Fungal Flavoenzyme Acting on Polyunsaturated Alcohols. *Biochem. J.* **2005**, *389*, 731−738.
(54) Matthews, S.; Tee, K. L.; Rattray, N. J.; McLean, K. J.; Leys, D.; Parker, D. A.; Blankley, R. T.; Munro, A. W. Production of Alkenes and Novel Secondary Products by P450 OleTJE Using Novel H2O2-Generating Fusion Protein Systems. *FEBS Lett.* **2017**, *591*, 737−750.
(55) Beyer, N.; Kulig, J. K.; Fraaije, M. W.; Hayes, M. A.; Janssen, D. B. Exploring PTDH−P450BM3 Variants for the Synthesis of Drug Metabolites. *ChemBioChem* **2018**, *19*, 326−337.
(56) Poraj-Kobielska, M.; Kinne, M.; Ullrich, R.; Scheibner, K.; Kayser, G.; Hammel, K. E.; Hofrichter, M. Preparation of Human Drug Metabolites Using Fungal Peroxygenases. *Biochem. Pharmacol.* **2011**, *82*, 789−796.
(57) Kiebist, J.; Holla, W.; Heidrich, J.; Poraj-Kobielska, M.; Sandvoss, M.; Simonis, R.; Gröbe, G.; Atzrodt, J.; Hofrichter, M.; Scheibner, K. One-Pot Synthesis of Human Metabolites of SAR548304 by Fungal Peroxygenases. *Bioorg. Med. Chem.* **2015**, *23*, 4324−4332.
(58) Kiebist, J.; Schmidtke, K.-U.; Zimmermann, J.; Kellner, H.; Jehmlich, N.; Ullrich, R.; Zänder, D.; Hofrichter, M.; Scheibner, K. A Peroxygenase from Chaetomium Globosum Catalyzes the Selective Oxygenation of Testosterone. *ChemBioChem* **2017**, *18*, 563−569.
(59) Fessner, N. D.; Srdič, M.; Weber, H.; Schmid, C.; Schönauer, D.; Schwaneberg, U.; Glieder, A. Preparative-Scale Production of Testosterone Metabolites by Human Liver Cytochrome P450 3A4. *Adv. Synth. Catal.* **2020**, *362*, 2725.
(60) Carro, J.; Ferreira, P.; Rodríguez, L.; Prieto, A.; Serrano, A.; Balcells, B.; Ardá, A.; Jiménez-Barbero, J.; Gutiérrez, A.; Ullrich, R.; Hofrichter, M.; Martínez, A. T. 5-Hydroxymethylfurfural Conversion by Fungal Aryl-Alcohol Oxidase and Unspecific Peroxygenase. *FEBS J.* **2015**, *282*, 3218−3229.
(61) Alcalde, M. Mutagenesis Protocols in Saccharomyces Cerevisiae by In Vivo Overlap Extension. In *Vitro Mutagenesis Protocols*, 3rd ed; Braman, J., Ed.; Humana Press: Totowa, NJ, 2010; Vol. *634*; pp 3−14.

https://dx.doi.org/10.1021/acscatal.0c03029
ACS Catal. 2020, 10, 13524−13534